Journal of the Energy Institute 125 (2026) 102447

Contents lists available at ScienceDirect

Journal of the Energy Institute

journal homepage: www.elsevier.com/locate/joei

Comparative study of the effects of reactor system and catalysts on glycerol valorisation via aqueous-phase reforming

Carine T. Alves [a,2,1], Francisco Maldonado-Martín [b,1], Alejandro Lete [b], Seyed Emad Hashemnezhad [a], Lucía García [b,*], Jude A. Onwudili [a]

[a] Energy and Bioproducts Research Institute, Aston University, Birmingham, B4 7ET, West Midlands, United Kingdom
[b] Thermochemical Processes Group (GPT), Aragon Institute of Engineering Research (I3A), Universidad de Zaragoza, Mariano Esquillor S/N, 50018, Zaragoza, Spain

ARTICLE INFO

Keywords:
Glycerol
Heterogeneous catalysis
Aqueous phase reforming
Hydrogen
Batch reactor
Fixed-bed reactors

ABSTRACT

The conversion of glycerol through aqueous phase reforming (APR) presents an important opportunity for sustainable chemical and fuel production. This study explores the APR of glycerol using three catalysts (nickel supported on alumina (NiAl), copper supported on alumina (CuAl), and bimetallic nickel-iron supported on alumina (NiAlFe)), synthesized via the coprecipitation method. The APR experiments were conducted in both batch and fixed-bed reactors. In the batch reactor, a 75 mL Parr reactor was utilised, operating at 238 °C and 5 bar initial nitrogen pressure with 20 mL of a 5 wt% glycerol solution and 0.3 g of catalyst (catalyst/glycerol mass ratio = 0.3). The fixed-bed reactor was made of a stainless steel tube loaded with 2 g of catalyst, operating at 238 °C and 37 bar, with a continuous feed of 5 wt% glycerol solution, equivalent to catalyst/glycerol mass ratio of 0.33. NiAl produced the highest conversion of glycerol to gases and the highest yield of hydrogen (230 mg H_2/mol C fed). However, among the tested catalysts, NiAlFe demonstrated superior performance, achieving a carbon yield to total products (liquid and gases) of approximately 80 % in the batch reactor as well as a relatively high hydrogen yield (141 mg H_2/mol C fed). These results underscore the promising potential of the NiAlFe catalyst for efficient glycerol conversion in APR processes, paving the way for advancements in sustainable fuel and chemical production.

1. Introduction

The increasing global demand for sustainable and renewable energy and organic chemical sources has intensified research into the development of technologies for targeted valorisation of biomass and biomass-derived feedstocks. Among these feedstocks, glycerol, a major by-product of biodiesel production via transesterification, emerges as an economically and environmentally attractive option. Its high availability, low cost, and versatility as a precursor for hydrogen production and fine chemical synthesis make it particularly promising. As the biodiesel industry continues to expand, the surplus of glycerol requires innovative technologies for its effective utilisation [1,2].

Over the last two decades, aqueous phase reforming (APR) has emerged as a promising technology, involving the catalytic conversion of biomass and biomass-derived feedstocks like glycerol to produce hydrogen in hot-pressurized water media. In addition, hydrogenolysis of glycerol under similar aqueous reaction conditions to APR can yield high-value organic compounds. Both APR and hydrogenolysis are operated under milder conditions compared to traditional steam reforming or pyrolysis, making them more energy-efficient and well-suited for decentralized hydrogen and chemicals production. Both APR and hydrogenolysis present several advantages, including lower operational temperatures (200–300 °C) and moderate pressures, resulting in reduced energy input [2].

Typically, the APR reaction mechanism includes glycerol degradation followed by a water-gas shift reaction, ideally generating 7 mol of hydrogen and 3 mol of carbon dioxide for every mole of glycerol consumed as shown in Equation (1) [3].

$$C_3H_8O_3 + 3H_2O \rightarrow 3CO_2 + 7H_2 \quad (1)$$

While noble metal catalysts like platinum and rhenium have been

* Corresponding author.
E-mail address: luciag@unizar.es (L. García).
[1] These authors contributed equally to this work.
[2] Permanent address: Energy Engineering Department, Universidade Federal do Reconcavo da Bahia, CETENS, Feira de Santana 44.085–132, Brazil.

https://doi.org/10.1016/j.joei.2026.102447
Received 12 November 2025; Received in revised form 2 January 2026; Accepted 6 January 2026
Available online 10 January 2026

extensively studied for this reaction, their high cost and limited availability pose challenges for scalability [2,4–6]. Therefore, nickel-based catalysts have gained attention as promising alternatives due to their high catalytic activity, lower costs, and ability to operate efficiently under APR conditions while minimizing severe coke formation, which is a frequent issue with other metal catalysts [7]. However, supported Ni-based catalysts have been reported to deactivate rapidly at APR conditions of 225 °C and 22 bar [8]. Researchers have been investigating modifications to these catalysts, such as bimetallic or alloyed systems, to enhance their stability and selectivity. For example, integrating iron and copper into nickel-based catalysts has demonstrated improved hydrogen selectivity, reduced carbon deposition, and increased catalyst longevity in APR processes [5,6].

On the other hand, glycerol hydrogenolysis involves cleaving C-C and C-O bonds in glycerol to yield valuable chemicals like 1,2-propanediol, ethylene glycol, and methanol. This process can proceed with or without additional hydrogen. Utilizing nickel-based catalysts for hydrogenolysis is particularly appealing, as they can generate hydrogen in situ through glycerol reforming, thus eliminating the need for external hydrogen sources [5,9]. The incorporation of iron in nickel-aluminium catalysts has been shown to enhance both catalytic activity and selectivity for desired products [10].

Recent studies have sought to optimize nickel-based catalysts by modifying their composition and preparation methods. For instance, the addition of iron into nickel-aluminium catalysts improves their reducibility and catalytic performance during the reforming of hydrocarbons [10]. Furthermore, the calcination temperature of these catalysts significantly influences their structural properties and catalytic efficiency. For example, Raso et al. [11] observed that, within the 500–750 °C range, the Ni/Al_3Fe_1 catalyst calcined at 625 °C exhibited the best catalytic performance, attributed to an optimal balance of acidity and metal dispersion. In contrast, further increasing the calcination temperature to 750 °C resulted in a decrease in total acidity and glycerol conversion in the aqueous-phase hydrogenolysis of glycerol [11]. Bimetallic catalysts, such as Ni-Cu and Ni-Fe, are also being explored for glycerol conversion processes, providing a combination of nickel's high activity with the enhanced selectivity and stability offered by the second metal [12]. Studies indicate that bimetallic Ni-Cu catalysts outperform their monometallic counterparts in both APR and hydrogenolysis reactions of glycerol, demonstrating improved hydrogen selectivity and reduced coke [13].

In this present work, the effect of catalyst compositions and the experimental reactor system, (batch and fixed-bed) on glycerol conversion via APR and hydrogenolysis have been studied. For the fixed-bed reactor reaction conditions were fixed at 238 °C and 37 bar, while for the batch reactor, the same temperature was used with slightly different autogenic pressures recorded. Three catalysts prepared by coprecipitation: NiAl, CuAl and NiFeAl have been used in this study. Detailed characterisations of the reaction products and spent catalysts have been carried out to determine the optimum conditions for production of hydrogen and/or value-added chemicals from chemicals. The influence of the operational differences between the batch reactor and the fixed bed continuous reactor on the experimental results would provide further insights into their applicability for effective glycerol valorisation.

2. Material and methods

2.1. Materials

Glycerol with high purity (+99 %, Fisher Scientific or +99.5 %, Sigma-Aldrich) was purchased and used as received. The 5 wt% glycerol feedstock was prepared by dissolving a known amount of glycerol in deionized water obtained either from an in-house Milli-Q Advantage A10 purification system or Milli-Q water supplied by Sigma-Aldrich. The glycerol (Fisher Scientific), ethanol (EtOH) (98 %, Fisher Scientific), acetic acid glacial (extra pure, Fisher Scientific), 1,2-propanediol (1,2-PDO) (99 %, extra pure, Thermo Scientific Chemicals), ethylene glycol (99 %, Thermo Scientific Chemicals), acetol (95 %, Thermo Scientific Chemicals), were employed to prepare solutions for the calibration curves for analysis of liquid samples by HPLC.

To complement the HPLC analysis, glycerol (Sigma-Aldrich), EtOH (>99.5 %, Sigma-Aldrich), acetic acid glacial (100 %, Merk), 1,2-PDO (≥99.5 %, Merk), acetol (90 %, Merk), ethylene glycol (≥99.5 %, Merk), acetone (≥99.9 %, Carlo Erba), methanol (≥99.9 %, Carlo Erba), acetaldehyde (≥99.5 %, Sigma-Aldrich), isopropanol (≥99.8 %, ChemLab), and 1-butanol (≥99.5 %, PanReac) were used to prepare solutions for calibrating GC-FID for the analysis of liquid samples. Gas products generated in the batch reactor were collected using 1 L Tedlar sampling bags (Restek, Saunderton, UK) for analysis.

2.2. Catalyst preparation and characterization

Three catalysts, NiAl, CuAl, and NiAlFe, were prepared by the coprecipitation method. The NiAl catalyst was prepared with the theoretical molar ratio Ni/(Ni + Al) to give 28 molar % of Ni following the procedure previously described [14]. The final calcination temperature was 675 °C. The ICP-OES analysis determined a molar % Ni of 28.3 %, which was very close to the theoretical value. The surface area of the NiAl catalyst had previously be determined to be 203 $m^2\ g^{-1}$ [15]. The CuAl catalyst was prepared with the theoretical molar ratio Cu/(Cu + Al) to also give 28 molar % of Cu following a previous procedure [15] but modifying the final pH at 6 and without the step of filtration and washing the precipitate prior to drying. The final calcination temperature was 675 °C. This allowed the Cu content in the calcined catalyst to reach 26.5 wt% and a surface area of 168 $m^2\ g^{-1}$ [16]. The NiAlFe catalyst was synthesized with a 28 mol% of Ni in Ni + Al + Fe and an Al/Fe molar ratio of 3:1 and calcined at a final temperature of 625 °C [11]. The measured contents of Ni and Fe were 26.8 mol% and 17.7 mol %, respectively, which were similar to the theoretical formulation. The surface area of the calcined catalyst was 199 $m^2\ g^{-1}$ [11]. More data about characteristics of the catalysts can be found in Table 1.

The reducibility study of calcined catalysts was carried out by H_2-TPR and optimized to fix the reduction temperature of NiAl catalyst at 700 °C, 260 °C for the CuAl catalyst, and 500 °C for the NiAlFe catalyst [11,15].

2.3. Batch reactor procedure

A schematic overview of the glycerol APR procedure in a batch reactor is provided in Fig. 1.

The overall methodology has been described in detail in previous studies [9,17,18]. APR of glycerol was conducted in a 75 mL Parr batch

Table 1
Prepared catalysts and main characteristics.

Catalyst	Calcination temperature (°C)	S_{BET} (m^2/g)	V_p (cm^3/g)	d_p (nm)	Crystalline phases in reduced catalyst	NH_3 desorption (μmol/g cat)
NiAl [15]	675	203	0.19	3.9	Ni, $NiAl_2O_4$	555.7
CuAl [16]	675	168	0.36	8	Cu	1390.4[a]
NiAlFe [11]	625	199	0.17	3.9	$FeNi_3$, $AlNi_3$, $NiAl_2O_4$, $FeAl_2O_4$	881.5

[a] Data from reference [15].

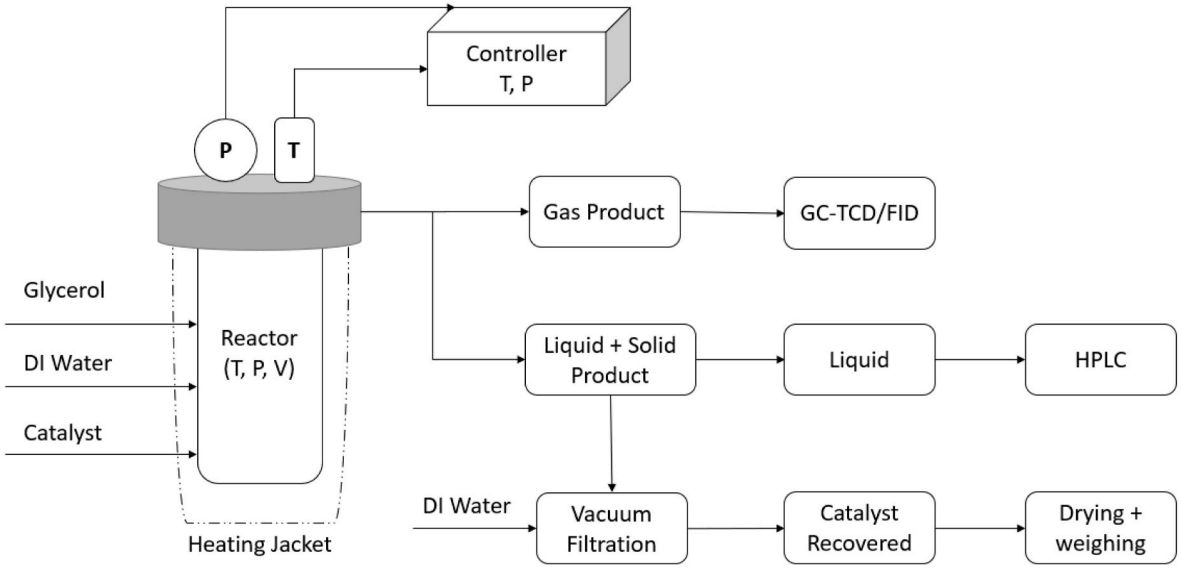

Fig. 1. Schematic representation of the batch reactor process for APR of glycerol.

reactor. Each run used a 5 wt% glycerol solution, prepared by mixing 1 g glycerol with 19 g deionized water, and 0.3 g of catalyst. Prior to reaction, the catalyst was reduced under 100 cm^3 (STP) min^{-1} hydrogen flow at temperatures determined by H_2-TPR for 1 h. This pre-treatment ensured catalyst activation before initiating the APR process. After sample introduction, the reactor vessel was sealed, flushed repeatedly with nitrogen (three cycles), and finally brought to 5 bar pressure using nitrogen. Nitrogen served to maintain an inert environment, enable reliable pressure measurements, and provide consistency for gas-phase analysis.

An electrically heated jacket raised the reactor temperature to 238 °C, at ~10 °C min^{-1}. After each run, the vessel was cooled to ambient within 30 min using a high-capacity fan. Post-cooling, pressure and temperature were recorded, gaseous products collected in 1 L Tedlar bags, and the slurry was vacuum-filtered through Whatman Grade 4 paper. The reactor was rinsed four times with 5 mL deionized water to ensure complete recovery. The recovered catalyst was dried at 105 °C overnight and weighed for mass balance. Liquid products were analysed via HPLC. Replicated runs showed <5 % standard deviation in glycerol conversion and gas yield, confirming reproducibility.

2.3.1. Analysis of gas-phase products from batch reactor

The procedure adopted for gas-phase analysis in this work was based on methods previously validated and reported in the literature [9,13,18]. Gas samples were analysed using a Shimadzu GC-2014 gas chromatograph. For each analysis, 0.6 mL of gas was withdrawn with a gas-tight syringe and injected into the instrument. The injector temperature was fixed at 60 °C, while detection was carried out using a flame ionization detector (FID) and a thermal conductivity detector (TCD), both maintained at 220 °C. The oven program commenced at 80 °C, followed by heating to 180 °C at a rate of 10 °C min^{-1}, with an isothermal hold of 3 min, giving a total run time of 13 min. Hydrocarbons were separated on a Hayesep column (80–100 mesh, 2 mm internal diameter, 2 m length) and quantified with the FID. Permanent gases (H_2, N_2, CO_2, and CO) were analysed using a molecular sieve column (60–80 mesh, 2 mm internal diameter, 2 m length) quantified with the TCD.

The general gas equation in Equation (2) was used to calculate the mass of each gaseous species from its volume fraction obtained by GC:

$$\text{Mass of each gas component, } m_i = \left(\frac{P_i \times V \times M_i}{RT}\right) \quad (2)$$

where m_i is the mass of species i (g), P_i is its partial pressure (calculated from the volume fraction and reactor pressure after cooling, Pa), V is the reactor headspace volume (m^3), M_i is its molar mass (g mol^{-1}), R is the universal gas constant (8.314 J mol^{-1} K^{-1}), and T is the post-cooling reactor temperature (K).

The carbon yield to gases was defined according to Equation (3):

$$\text{Carbon yield to gases (\%)} = \frac{\text{C moles in the gas products}}{\text{C moles in the glycerol feed}} \times 100 \quad (3)$$

The H_2 yield was calculated according to Equation (4):

$$\text{Hydrogen yield}\left(\frac{\text{mg } H_2}{\text{mol C fed}}\right) = \frac{n_{H_2} MW_{H_2} \times 1000}{\text{C moles in the glycerol feed}} \quad (4)$$

where n_{H_2} are the moles of H_2 (mol), and MW_{H_2} is the molecular weight of H_2 (g mol^{-1}).

Since the gaseous products were kept under pressurized nitrogen (about 5–6 bar), the amount of dissolved CO_2 was corrected using Henry's law [19].

2.3.2. Analysis of liquid-phase products from batch reactor

Liquid effluents collected from the reactor were analysed by High-Performance Liquid Chromatography (HPLC) for both identification and quantification of the soluble compounds [17]. The chromatographic runs were carried out using an Agilent 1260 Infinity HPLC unit fitted with a quaternary pump, an autosampler, a diode array detector (DAD), and a refractive index detector (RID). Separation of the compounds was achieved using an Agilent Hi-Plex H column (300 × 7.7 mm, 8 μm). Prior to chromatographic analysis, all samples were passed through a PTFE syringe filter of 0.2 μm pore size in order to eliminate suspended particles.

Adequate amount of water (20 mL) was used to recover the reactor effluents after each experiment and no further dilution was necessary prior to HPLC analysis. The HPLC eluent consisted of an aqueous solution of H_2SO_4 at 5 mM concentration with a 0.5 mL min^{-1} flow rate. The chromatographic column was kept at 25 °C, and 20 μL of each sample was injected. Compound detection was performed by the DAD at 210 nm together with the RID.

Calibration standards were prepared from pure reference chemicals (glycerol, EtOH, acetic acid, ethylene glycol, 1,2-PDO, and acetol) and analysed under identical chromatographic conditions to generate calibration curves. The calibration curves exhibited excellent linearity, with correlation coefficients (R^2) greater than 0.99. Quantification of the liquid components was performed through peak area comparison with

standard solutions, and retention times were used to validate compound assignment.

The conversion of glycerol was calculated using Equation (5):

$$\text{Glycerol Conversion (\%)} = \frac{\text{mole of glycerol feed} - \text{mole of unreacted glyclerol}}{\text{mole of glycerol feed}} \times 100 \quad (5)$$

The carbon yield to liquids is calculated according to Equation (6):

$$\text{Carbon yield to liquids (\%)} = \frac{2n_{EtOH} + 2n_{Acetic\ Acid} + 3n_{Acetol} + 3n_{1,2-PDO} + 2n_{Ethylene\ glycol}}{\text{C moles in the glycerol feed}} \times 100 \quad (6)$$

2.4. Fixed-bed reactor procedure

A schematic overview of the glycerol APR procedure in a fixed-bed reactor is provided in Fig. 2 [20].

The catalytic fixed-bed reactor studies were conducted in a laboratory-scale continuous feeding system from "Process Integral Development Eng & Tech (PID, Spain)". The system consisted of a stainless-steel tubular reactor, designed and developed by Autoclave Engineers, with an inner diameter of 9 mm and a length of 250 mm. Inside the reactor is placed a fixed bed of 5.5 cm^3, which consists of a mixture of 2 g of catalyst (particle size 160–315 μm) and the desired amount of inert sand to reach the mentioned bed volume. Before each reaction, the catalyst was reduced according to the H_2-TPR results previously cited by employing an H_2 stream of 100 cm^3 (STP) min^{-1} for 1 h.

The reaction was carried out at the selected reaction conditions (238 °C, 37 absolute bar) for 2 h. The set of reaction conditions were based on previous optimisation studies using the fixed-bed reactor [12]. Feeding of the solution was started after carrying out a stabilization procedure. When temperature and pressure reached values closed to reaction conditions, the 5 wt% of glycerol solution in Milli-Q water was fed using a high-performance liquid chromatography (HPLC) pump and the experiment began. For this fixed-bed reactor process, the catalyst weight/glycerol flow rate ratio was 40 g catalyst min g $glycerol^{-1}$, which was equivalent to catalyst/glycerol mass ratio of 0.33. The system pressure was maintained employing an Equilibar LP Series Precision Back Pressure Regulator.

The exit stream was directed through a back-pressure regulator, depressurized, and subsequently passed to a condensation train consisting of four condensers immersed in an ice bath. The initial condenser collected water released during reaction stabilization, the second and third collected liquid products formed during reaction (1 h per condenser). More details about the experimental procedure can be found in previous studies [11,12,15,20].

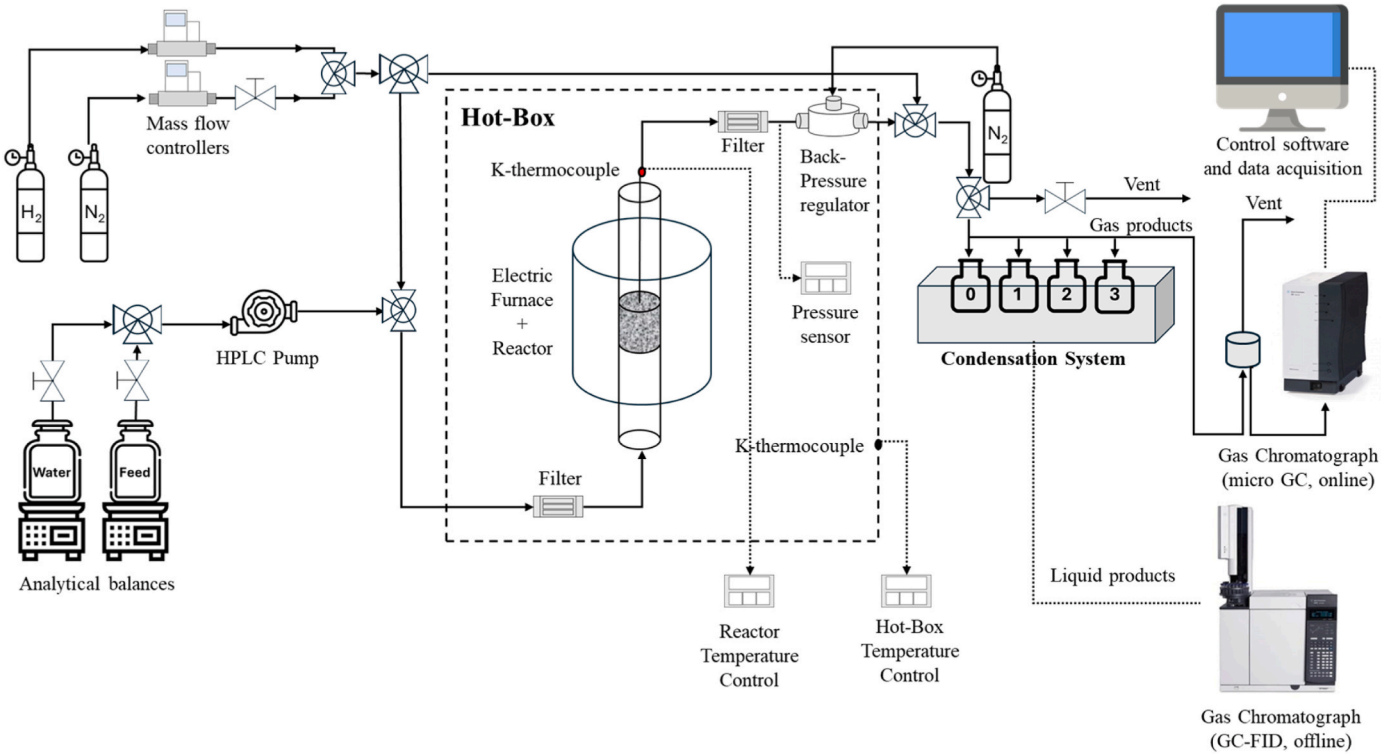

Fig. 2. Schematic representation of the fixed-bed reactor process for APR of glycerol.

2.4.1. Analysis of gas-phase products from fixed-bed continuous reactor

Gas-phase products were analysed online using a micro-GC (Agilent 490 Micro GC) equipped with two different modules. Channel A contains a Plot U column with a TCD, where CO_2, C_2H_6, and C_3H_8 were detected and quantified using helium as carrier gas. Channel B with a molecular sieve column and a TCD was used to analyse H_2, N_2, CH_4, and CO with argon as carrier gas.

In most experiments, an N_2 gas flow of 75 cm^3(STP) min^{-1} was fed by a mass flow controller (Hi-Tec Bronkhorst), downstream of depressurization, and was used as an internal standard. The injector's temperature of both columns was set at 110 °C. The analysis conditions for the molecular sieve column were set at 90 °C and 150 kPa, while the conditions for the Plot U column were set at 100 °C and 150 kPa. Each analysis had a duration of less than 3 min.

The gas analyses during the second hour of the experiment were employed to quantify the gas production. The flow rate of each product gas was determined from the percentage volume obtained by the micro-GC analysis and the flow rate of N_2 used as an internal standard. The molar flow rate of each product gas was calculated by dividing the volumetric flow rate (STP) by the volume of 1 mol (STP). The integration of the molar flow rate determines the moles of each product gas during this time interval.

The carbon yield to gases (%) and hydrogen yield (mg H_2/mol C fed) was calculated with similar equations (3) and (4) respectively, considering the glycerol feed during the second hour of the experiment. In this time interval, the system is stationary without the effect of the death time.

2.4.2. Analysis of liquid-phase products from fixed-bed continuous reactor

The liquid products collected in the condensation system during the second hour of each experiment were analysed off-line with an Agilent 7820 A GC, which was configured with a FID and an Agilent HP-FFAP 19091F-105 capillary column. The products detected and quantified were acetaldehyde, acetone, methanol, isopropanol, EtOH, acetol, acetic acid, 1,2-PDO, ethylene glycol, and unreacted glycerol. To reduce the error derived from the sample injection variations, 1-butanol was used as an internal standard. The injector and detector temperatures were 275 °C and 300 °C, respectively. Each sample was analysed three times to increase the results accuracy.

Standard mixtures of accurately known concentrations of the relevant compounds were made from pure compounds, and 1-butanol was used as an internal standard for response factor determination.

Because the glycerol analysis in liquid samples was not reliable, probably due to some retention in the capillary column, glycerol conversion was not employed and was used carbon yield to total products (Equation (7)).

$$\textit{Carbon yield to total products}\ (\%) = \textit{Carbon yield to gases}\ (\%) + \textit{Carbon yield to liquids}\ (\%) \quad (7)$$

The definition of carbon yield to liquids is similar to Eq. (6) for the batch system. However, in the fixed-bed continuous system, more compounds were considered in the calibration.

3. Results

3.1. Carbon yield to products

Fig. 3 shows the results of carbon yield to gases in batch and fixed bed reactors. For both reactors, the CuAl catalyst generated by far the lowest yields of gases with carbon, less than 1 %. Catalysts with Ni in their composition, NiAl, and NiAlFe, showed values around 12 %, except almost 21 % for the NiAl catalyst in the batch system. The different performance of Ni and Cu as active metals in the reaction of glycerol conversion by APR could be linked to the ability of Ni to break C-C bonds, which Cu does not possess [21]. For both NiAl and NiAlFe catalysts, the different performances of the two reactor could be ascribed to possible secondary reactions in the batch reactor due to both the extended reactor heat up and reaction times compared to the fixed-bed reactor. However, results showed that the NiAl was more active towards secondary reactions than NiAlFe, indicating that the Fe suppressed Ni's ability for C-C bond breaking.

Fig. 4 shows the results of carbon yield to liquids. The CuAl catalyst showed lowest values of around 8 %, with similar yields in both the batch and fixed bed reactors. Similar to the results for gas-phase products, both Ni-based catalysts showed higher carbon yield to liquids in batch reactor than in fixed bed reactor. For both reactors, the NiAlFe catalyst generated higher carbon yield to liquids than the NiAl catalyst. Thus, the carbon yield to liquids obtained with NiAlFe catalyst in batch reactor was approximately 65 %, while for this catalyst in fixed bed reactor was 57.3 %.

The presences of the phases $FeNi_3$ and $AlNi_3$ in the NiAlFe catalyst have been identified to have a relevant role in increasing the catalytic activity toward liquid products formation, glycerol conversion, and yield of 1,2-PDO [14]. The higher carbon yield to liquids in batch reactor than in fixed bed reactor could be a consequence of the different flow

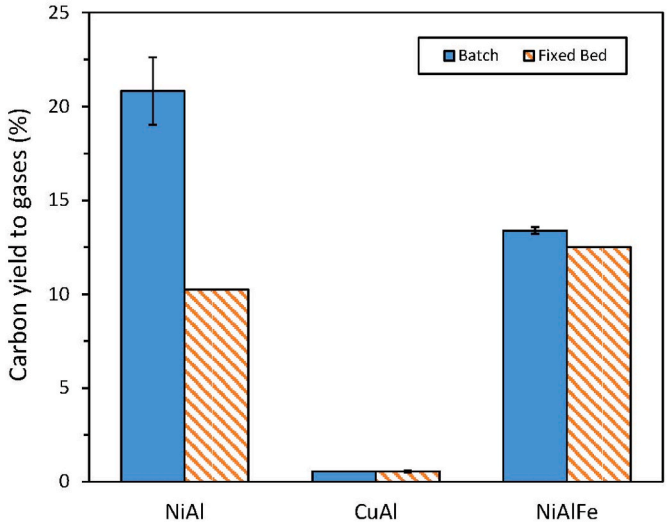

Fig. 3. Carbon yield to gases with NiAl, CuAl, and NiAlFe catalysts using batch and fixed bed reactors.

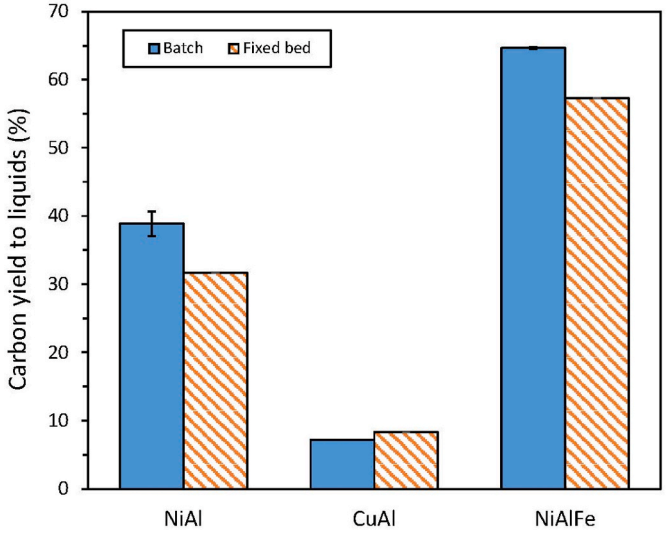

Fig. 4. Carbon yield to liquids with NiAl, CuAl, and NiAlFe catalysts using batch and fixed bed reactors.

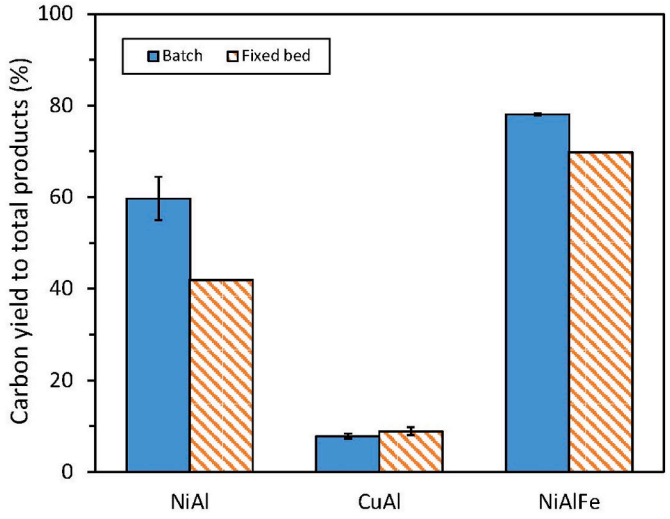

Fig. 5. Carbon yield to total products with NiAl, CuAl, and NiAlFe catalysts using batch and fixed bed reactors.

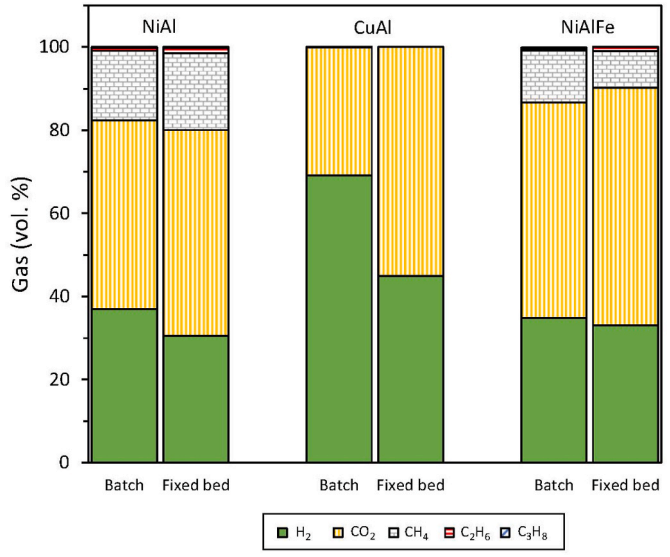

Fig. 6. Gas composition with NiAl, CuAl, and NiAlFe catalysts using batch and fixed bed reactors.

pattern as is explained in detail in the Discussion section.

For each catalyst and reactor type, carbon yield to liquids was higher than carbon yield to gases. This indicated that at the operating conditions selected, 238 °C and 37 bar, glycerol was mainly converted to liquids, indicating that APR conditions can be suitable for producing sustainable chemicals from glycerol [12]. These operating conditions could be optimized to shift the selectivity of reaction products either towards gas or chemical production, respectively. As a test, the glycerol feed was previously reacted over the NiAlFe catalyst in a fixed bed reactor at 227 °C and 34 bar and the results obtained were around 10 % of carbon yield to gases and around 38 % of carbon yield to liquids [11]. These results are lower than those obtained in the present study at 238 °C and 37 bar, especially the carbon yield to liquids but still indicated the high conversion to liquids in the presence of the NiAlFe catalyst compared to NiAl and CuAl.

Fig. 5 shows the results of carbon yield to total products. The NiAlFe catalyst showed the highest yield in both reactors, followed by the NiAl catalyst. The carbon yield to total products was close to 80 % using the NiAlFe catalyst in the batch reactor. The yield obtained with the CuAl catalyst was the lowest, remaining below 9 %.

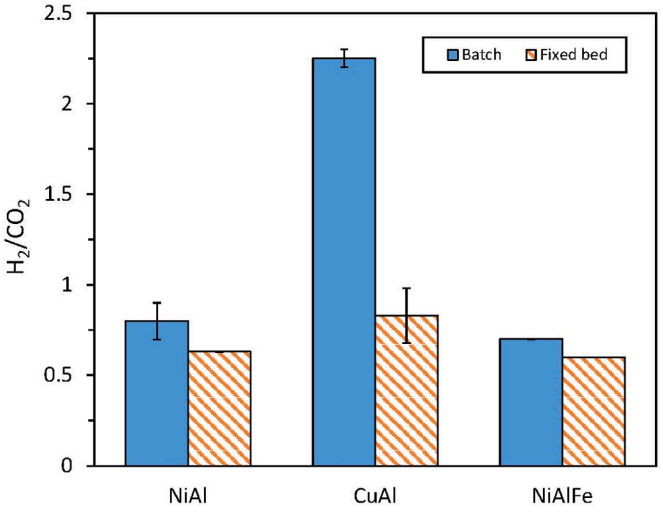

Fig. 7. Molar H_2/CO_2 ratio in the gas phase with NiAl, CuAl, and NiAlFe catalysts using batch and fixed bed reactors.

3.2. Gas phase

Fig. 6 shows gas composition expressed as volume percentage. CO_2 was the gas component with the highest content in most cases, followed by H_2 and CH_4. Low contents of C_2H_6 and C_3H_8 were also quantified. The gas phase obtained with the CuAl catalyst was composed mostly of CO_2 and H_2 and negligible amounts of other gases. An exception was the higher content of H_2 (69.1 vol%) than CO_2 (30.9 vol%) for the batch reactor using the CuAl catalyst. The absence of CH_4, C_2H_6 and C_3H_8 in the gas phase generated using the CuAl catalyst could be explained to the poor ability of CuAl catalyst to break C-C bonds [21]. CH_4 content in gas phase was smaller when using the NiAlFe catalyst than the NiAl catalyst. The general trend showed that H_2 content was higher in the gas phase of batch reactor than of fixed bed reactor for each catalyst. The differences between H_2 content in batch reactor compared to fixed bed reactor are significant for the CuAl catalyst and small for the NiFeAl catalyst, while the NiAl catalyst shows an intermediate performance.

Fig. 7 shows the molar H_2/CO_2 ratio in the gas phase. The values were close to 0.8 and 0.6 for the NiAl catalyst for batch and fixed bed reactors, respectively. Different values of the molar H_2/CO_2 ratio were obtained for the CuAl catalyst. In the batch reactor, the molar H_2/CO_2 ratio was 2.25 very close to 2.33 (7/3), the theoretical value of glycerol steam reforming to CO_2 and H_2 (Equation (1)). However, the molar H_2/CO_2 ratio for the CuAl catalyst in the fixed bed reactor was 0.83. Cu is a metal that shows high activity for water-gas shift reaction [21]. Moreover, the flow pattern in batch reactor with high stirring could remove hydrogen from the catalyst surface avoiding hydrogenation reactions. These two facts could explain the high H_2/CO_2 ratio observed in batch reactor using the CuAl catalyst.

The molar H_2/CO_2 ratio obtained with the NiAlFe catalyst showed lower values, 0.7 and 0.6 for batch and fixed bed reactors respectively. These values of the molar H_2/CO_2 ratio could indicate the participation of NiAlFe catalyst in hydrogenation reactions decreasing the content of hydrogen in the gas phase. The molar H_2/CO_2 ratio was higher for batch reactor than fixed bed reactor for each catalyst. So far, results have shown NiAl and NiAlFe catalysts were more active than CuAl catalyst and as a consequence, they generated more gases as evidenced by the increase the final gas pressure in the batch reactor (6 bar for CuAl; 10.5 bar for NiAl; and 8.8 bar for NiAlFe). The higher reaction pressure in the batch reactor, up to 42.8 bar for the NiAl catalyst, than in the fixed bed reactor, 37 bar, could produce higher carbon yield to gases [22]. The increase of total pressure should increase CO_2 solubility, and the CO_2

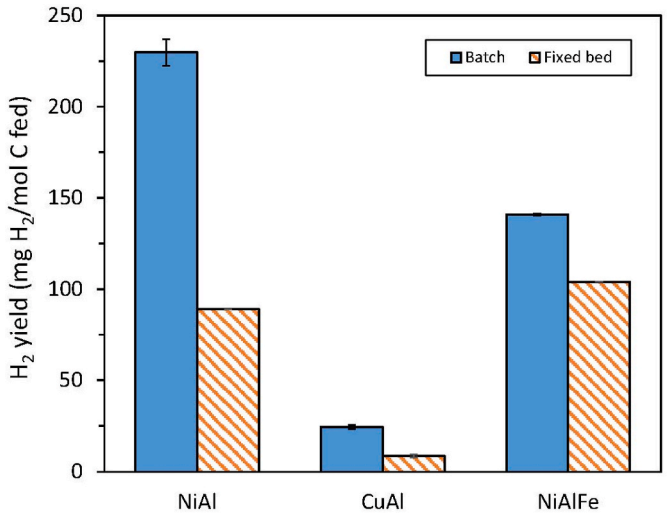

Fig. 8. H_2 yield with NiAl, CuAl, and NiAlFe catalysts using batch and fixed bed reactors.

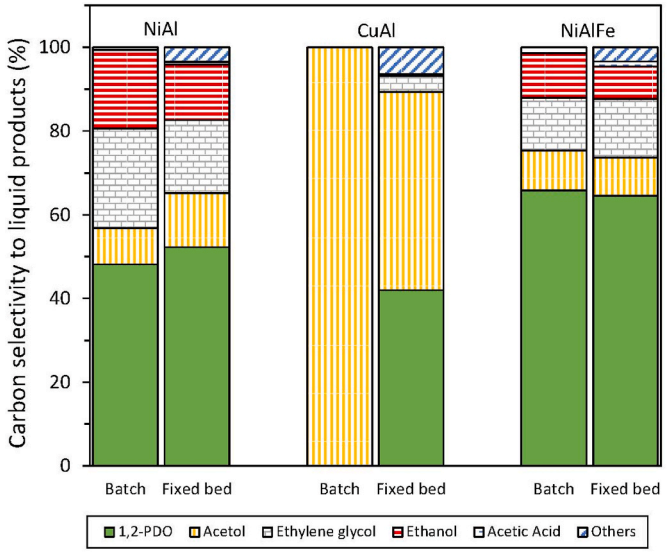

Fig. 9. Carbon selectivity to liquid products with NiAl, CuAl, and NiAlFe catalysts using batch and fixed bed reactors.

content would decrease in the batch reactor. Moreover, considering the flow pattern in batch reactor; high stirring rate would translate to higher value of mass transfer coefficient in the liquid-solid film, which could remove hydrogen from the catalyst surface and hinder hydrogenation reaction of liquid products. In a fixed bed reactor, the regime of agitation would be caused by contact between the liquid stream and bubbles of product gases flowing across the catalyst bed. This should be deemed to be much lower compared to the stirring in the batch reactor, thereby helping to maintain hydrogen on the catalyst surface to enhance hydrogenation reactions in the fixed bed reactor.

Fig. 8 shows the H_2 yield, reported in mg H_2/mol C fed. The NiAl catalyst gave the highest yield of H_2 followed by the NiAlFe catalyst, both in batch reactor, and the lowest yields are obtained with the CuAl catalyst. H_2 yield for each catalyst was higher in the batch reactor than in the fixed bed reactor. These results corroborated the participation of secondary reactions (such as cracking, reforming of intermediates and dehydrogenation) could have occurred to a greater extent in batch reactor than in fixed bed reactor. The observations agreed with the high C-C cleaving ability of Ni, leading to more extensive secondary reactions of the intermediate products from the original glycerol. It also confirmed the suppression of C-C cleavage when Fe was incorporated to make the NiAlFe catalyst.

3.3. Liquid phase products

Fig. 9 shows the results of carbon selectivity to liquid products. The term "others" relates to minor products (methanol, acetaldehyde, acetone and isopropanol), which only analysed for the fixed-bed tests. The NiAlFe catalyst showed similar liquid products distribution for both reactors. The main liquid product was 1,2-PDO, followed by ethylene glycol, acetol, and EtOH. The 1,2-PDO selectivity was close to 65 % in both reactors with this catalyst. A slightly higher content of EtOH was obtained in the batch reactor than in the fixed bed reactor. EtOH has been identified as a liquid product in acetol APR when using high catalyst weight/acetol flow rate ratios in a fixed bed reactor [23]. Other researchers have also proposed ethanol as a product in the pathway of glycerol APR, both in route 1 (dehydrogenation of glycerol and decarbonylation to ethylene glycol and hydrogenation/dehydration to ethanol) and route 2 (dehydration of glycerol to acetol and hydrogenation to 1,2-PDO) [24].

NiAl catalyst showed slight differences in carbon selectivity to liquid products depending on the reactor. While, 1,2-PDO was the main liquid product in both reactors, the carbon selectivity to 1,2-PDO were 52.8 and 48.1 % for fixed bed and batch reactors, respectively. 1,2-PDO was followed by ethylene glycol, EtOH, and acetol. The order was the same for both reactors, but the total content of 1,2-PDO and acetol, products of route 2 was higher in fixed bed reactor (66.22 %) than in batch reactor (56.88 %). As a consequence, the products such as ethylene glycol and EtOH from route 1 were higher in batch reactor (42.54 %) than in fixed reactor (30.55 %). This is a simplification because of EtOH can also be a product of route 2, specially in batch reactor. However, it must be noted that the reaction severity would have been higher in the batch reactor compared to the fixed bed, due to extended heat up and reaction times, as previously mentioned.

CuAl catalyst showed different performance in carbon selectivity to liquid products from the NiAl and NiAlFe catalysts. Acetol was the main product with the CuAl catalyst for both reactors. In batch reactor, only acetol was produced, but in fixed bed reactor the carbon selectivity to acetol decreased to 47.4 %. In fixed bed reactor, the selectivity towards products from route 2, 1,2-PDO and acetol, was close to a total of 90 %. This result can be a consequence of the low ability of Cu in C-C bond breaking. The higher participation of hydrogenation reactions in a fixed bed reactor could explain the production of 1,2-PDO in this reactor. This is corroborated by the lower molar H_2/CO_2 ratio and H_2 yield in the fixed bed reactor.

Previous studies on glycerol conversion to acetol in fixed bed reactors using CuAl catalysts prepared by coprecipitation [15,20] have shown low glycerol conversion and a significant carbon selectivity to 1, 2-PDO. The hydrogenation of acetol to 1,2-PDO can be explained by the presence of ethylene glycol and methanol in the liquid products. Ethylene glycol is a product derived from glycerol by the dehydrogenation route and methanol is a product derived from ethylene glycol by decarbonylation-dehydrogenation [15]. Moreover, the formation of Cu_2O phase in the catalyst during the reaction could have a relevant role in the redox catalysis to convert acetol to 1,2-PDO [25].

The low activity shown by CuAl catalyst and the flow pattern, in a batch reactor with high agitation and a high value of mass transfer coefficient in the liquid-solid film can be relevant. This agitation could remove acetol from the catalyst surface together with the Cu species present in the reaction conditions (Fig. 10), could explain the absence of liquid products derived from the acetol reaction.

3.4. Characterization of spent catalysts

Despite the short reaction time used in the experiments, a

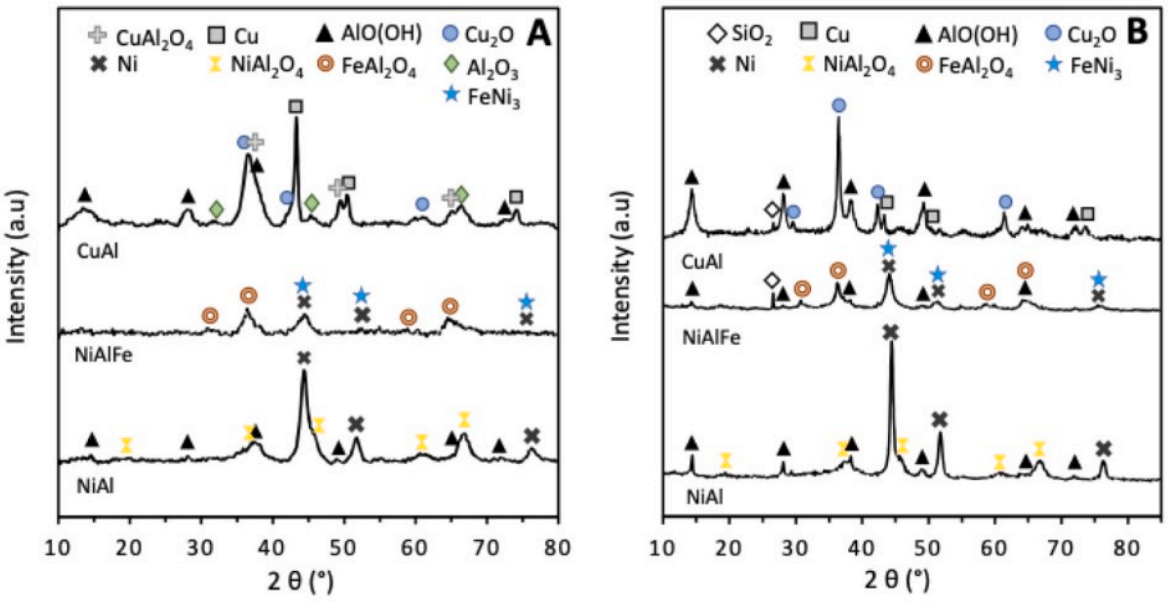

Fig. 10. XRD characterization of spent catalysts in batch reactor A), in fixed-bed reactor B).

Table 2
Carbon content in spent catalysts.

Catalyst	Reactor	C content (wt% ± SD)[a]
NiAl	Batch	1.49 ± 0.02
NiAl	Fixed-bed	0.85 ± 0.03
CuAl	Batch	2.21 ± 0.01
CuAl	Fixed-bed	1.25 ± 0.00
NiAlFe	Batch	2.05 ± 0.02
NiAlFe	Fixed-bed	1.08 ± 0.01

[a] Determined by elemental analysis; SD = Standard deviation.

characterization of the spent catalysts has been carried out to obtain some information on catalyst stability and the effect of reactor type. The results of carbon content determined by elemental analysis are shown in Table 2 and Fig. 10 presents the results of spent catalysts characterized by XRD.

The carbon content ranged from 1.49 wt% for NiAl to 2.21 wt% for CuAl in catalysts used in batch reactor and from 0.85 wt% for NiAl to 1.25 wt% for CuAl in catalysts employed in fixed-bed reactor. The slightly higher carbon level on CuAl suggests a marginally greater tendency for coking or strong tendence to adsorb organic residues compared with the Ni-based formulations. The carbon content follows the order NiAl < NiAlFe < CuAl for both reactors and could be related to catalyst acidity, with the CuAl catalyst having the highest value of catalyst acidity. The values of carbon content in spent catalysts used in batch reactor were higher than those in fixed-bed reactor. Even with the stirring, the batch reactor presented the tendency of glycerol and intermediate products to adsorb on the catalyst surfaces, polymerise and condensation into char. In addition, the composition of liquid-phase products from the batch reactor indicated that hydrogenation reactions were less effective in batch reactor, thereby leading to higher retention of organic residues on catalyst surface.

XRD results of spent catalysts showed the formation of new phases such as boehmite (AlO(OH)) and Cu_2O phase in the CuAl catalysts. The formation of boehmite via hydrothermal transformation of alumina ($Al_2O_3+H_2O \rightarrow 2$ AlO(OH)) has been widely reported when water is used as the reaction medium at elevated temperature and pressure [26,27]. Boehmite formation is known to modify surface area and acidity and, in severe cases, to significantly distort the catalyst structure, thereby affecting catalyst activity and selectivity [26]. However, the boehmite peaks observed in this present study were less intense than those reported in systems that suffered drastic deactivation. For both reactors, the catalysts showed the same tendency. The results clearly indicated that CuAl was susceptible to this transformation and that its hydrothermal stability would require further improvement. In contrast, the NiAl catalyst showed relatively stable structural properties with low intensity for boehmite peaks. The NiAlFe catalyst displayed the smallest intensity in boehmite peaks indicating superior structural stability compared with the other catalysts examined in this study. The higher intensity of boehmite peaks in fixed-bed reactor compared to batch reactor could be due to the higher contact time of the catalyst with water under the reaction conditions.

The formation of Cu_2O phase was in accordance with previous works of glycerol conversion in aqueous phase [15,20]. At the operating conditions metallic Cu is oxidised to Cu_2O. Different distribution of the oxidation states of the copper species in spent catalysts could be observed in this present study, depending on the reactor type. CuAl catalyst used in batch reactor showed Cu, $CuAl_2O_4$ and Cu_2O phases, while in fixed-bed reactor Cu_2O was the copper species with the highest intensity. This fact could explain the different gas and liquid product composition obtained, which could be corroborated by the work of Adrianto et al. [28], that showed the influence of the oxidation states of the copper species in glycerol transformation.

Catalyst stability is a relevant issue for a long-term process performance. Based on previous literature, the following facts should be considered regarding deactivation mechanisms. A previous work [29] carried out in fixed-bed reactor at 227 °C and 34 bar during 9 h using a NiAlFe catalyst calcined at 500 °C, concluded the formation of boehmite under reaction conditions without effect on glycerol conversion and carbon yield to gases and liquids. The $FeNi_3$ crystallite size was unaltered during all the experiment, but metal leaching occurred. Then, metal lixiviation was identified as main deactivation mechanism. In the present study, the calcination temperature of NiAlFe catalyst was 625 °C, which showed lower metal leaching than the catalyst calcined at 500 °C [11]. We propose future works to focus on catalyst stability to study the lixiviation of metals under operating conditions at longer reaction times.

4. Discussion

From the obtained results, a comparison between the NiAlFe and NiAl catalysts reveals several differences. On the one hand, the NiAlFe catalyst exhibited a higher carbon yield to liquids and a higher carbon selectivity to 1,2-PDO than the NiAl catalyst. On the other hand, the NiAl catalyst showed higher carbon yields to gaseous products in the batch reactor, a higher CH_4 content in the gas phase, and higher carbon selectivities to EtOH and ethylene glycol, which are products of route 1, compared to the NiAlFe catalyst. These differences can be explained by considering the catalyst characterization results. The textural properties of the catalysts cannot account for the observed trends, as both catalysts exhibit similar surface areas and pore diameters, with values of approximately 200 $m^2\ g^{-1}$ and 3.9 nm respectively [11,12]. In contrast, significant differences were observed in catalyst acidity. The NiAl catalyst, calcined at 675 °C, showed a total acidity of 555.7 μmol NH_3 g $catalyst^{-1}$ [12] whereas the NiAlFe catalyst, calcined at 625 °C, exhibited a substantialy higher total acidity of 881.5 μmol NH_3 g $catalyst^{-1}$ [11]. The higher acidity of the NiAlFe catalyst together with the highly dispersed $FeNi_3$ phase, can explain its higher carbon yield to liquids and enhanced hydrogenation capacity, leading to increased carbon selectivity towards 1,2-PDO.

Both reactors, batch and fixed bed, are multiphase reactors, with a solid (the catalyst), a liquid phase (containing glycerol and liquids products) and a gas phase (consisting of inert gas and gas products).

In the stirred batch reactor, the catalyst is suspended as a slurry by stirring. In contrast, the catalyst is static in fixed-bed reactor which is a bubble packed column, with up-flow of liquid and gas streams.

To analyse the conversion of glycerol, or the carbon yield to total products, only the flow patterns of liquid phase containing the glycerol reagent was considered in this present study. In the batch reactor, the liquid pattern could be modelled as a stirred-tank, while in the fixed-bed it could be assumed an ideal plug flow. As the gas generation increased, more gas bubbles would have existed the fixed-bed reactor, producing stirring effects on the liquid phase and increasing axial dispersion, thereby moving away from ideal plug flow.

To simplify liquid flow patterns for batch and fixed-bed reactors as stirred-tank and ideal plug pattern respectively, a parameter on importance would have been to compare the contact time. However, this would not be correct in this case because of the use of different catalyst mass and reactor volumes in both reactors. Therefore, in this case the adequate comparison for the same glycerol conversion in both reactors will be equation (8), where k* is the apparent constant of reaction rate, W is the catalyst mass (g), V is the reactor volume (mL), q_o is the feeding flow rate (mL/min) in the fixed-bed reactor and t (min) is the reaction time in the batch reactor, subscript FB is related for fixed-bed and subscript Batch is related for batch reactor.

$$k^*_{Batch}\frac{W_{Batch}}{V_{Batch}}t = k^*_{FB}\frac{W_{FB}}{q_o} \tag{8}$$

Assuming the V_{Batch} as the initial volume of the liquid phase and by entering the data, equation (9) was obtained:

$$k^*_{Batch}0.9 = k^*_{FB}2 \tag{9}$$

The apparent constant of reaction rate, k*, gave equation (10), considering that the intrinsic reaction rate is order 1 with respect to the glycerol concentration. This apparent constant reaction rate would include the intrinsic reaction rate and the mass transfer of glycerol through the liquid-solid film.

$$k^* = \frac{1}{\frac{f_s}{k_{Glys}a_s} + \frac{1}{k'\eta}} \tag{10}$$

The resistance of reaction rate, 1/(k'η), includes k', the constant of intrinsic reaction rate referred to mass of catalyst and the possible control of internal diffusion expressed by the efficient factor, η. The resistance of mass transfer in the liquid-solid film, includes f_s as the ratio W/V, k_{Glys}, which is the mass transfer coefficient in the liquid-solid film and a_s, the ratio of external surface of solid/V.

These explanations could help to analyse the obtained results. The effect of the catalyst in a specific reactor, for example batch reactor, influences k* through k'. Then, the low carbon yield to total products using the CuAl catalyst shown in Fig. 5 was due to the low value of k', indicating the catalyst activity for glycerol conversion. Therefore, the following order of catalyst activity could be proposed: NiAlFe > NiAl > CuAl. The same order was observed for fixed-bed reactor.

In order to analyse the impact of reactor type, two extremes of the value of k' could be considered. (1) In the case of a very low value of k' it could be considered that the global reaction rate was controlled by the intrinsic reaction rate. Then, if k* = k' and equation (9) predicts higher carbon yield to total products in fixed-bed reactor than in batch reactor. For the CuAl catalyst, Fig. 5 showed a slightly higher value of carbon yield to total products in fixed-bed reactor than in batch reactor, indicating a high control of reaction rate and a small influence of mass transfer in the liquid-solid film. Moreover, the different distribution of the oxidation states of the copper species (Fig. 10) could also influence on k'. (2) The case of a higher value of k' would produce a decrease of reaction rate resistance and an increase in the control of mass transfer resistance. The values of f_s for batch reactor and fixed-bed reactor could be estimated as 15 g/L and 364 g/L respectively. Moreover, experimental results showed that the term $k_{Glys}\ a_s$ for batch reactor would be higher than that for fixed-bed reactor due to the higher stirring in the former. As a consequence, the mass transfer resistance would be higher for fixed-bed reactor than for batch reactor with $k^*_{FB} < k^*_{Batch}$. This could explain the higher carbon yield to total products in batch reactor than in fixed bed reactor for NiAlFe and NiAl catalysts.

The results have shown higher hydrogen content, higher H_2/CO_2 ratio and higher H_2 yield in batch reactor than in fixed bed reactor for each catalyst. To explain these results, it has been proposed the different flow pattern in the two reaction systems. Moreover, the higher carbon yield to liquids in batch reactor than in fixed bed reactor could be due to also to the flow pattern. To corroborate these hypothesis, a new experiment with the NiAlFe catalyst in the fixed bed reactor maintaining the same operating conditions has been performed, but feeding the N_2 flow rate, 42 cm^3 (STP) min^{-1}, through the catalytic bed. The obtained results have shown the decrease of carbon yield to liquids, that could be due to the higher stirring due to the gas bubbles when a N_2 flow rate pass through the catalytic bed, moving away from the ideal plug flow decreasing glycerol conversion. The H_2/CO_2 ratio increases to 1.18, the H_2 gas composition reached 48.4 % and the H_2 yield was 259 mg H_2/mol C fed in this new experiment. The H_2 yield is the highest value determined in this work. Other results related to the liquid phase are: the carbon selectivity to 1,2-PDO decreases while carbon selectivity to acetol increases. These results could indicate that the flow of a N_2 flow through the catalytic bed would increase the mass transfer coefficient in the liquid-solid film that could help to remove acetol and hydrogen from the active sites in the catalyst inhibiting acetol reactions and hydrogenation reactions in liquid phase and increasing H_2 yield. Similar explanations have been done in the literature [30].

5. Conclusion

This present study has demonstrated that the reactor system, batch or fixed bed, has less influence than the catalyst in the conversion of glycerol by APR. Batch reactor showed slightly higher carbon yield to gases and liquids than fixed bed reactor for NiAl and NiAlFe catalysts, which could be due to flow pattern with high stirring that produced a higher value of the apparent constant of reaction rate due to small mass transfer resistance. The higher selectivity to hydrogenated products such as 1,2-PDO in fixed bed reactor than in batch reactor can be corroborated by the smaller hydrogen yield in fixed bed reactor than in batch reactor due to the participation of hydrogen in these reactions. Such

observation could be caused by the prevailing flow pattern in the reactors.

The experimental results indicate that the NiAlFe catalyst outperformed both NiAl and CuAl catalysts in terms of carbon yield to total products and structural stability. It achieved the highest carbon yield to total products (approximately 80 %) in the batch reactor. The NiAl catalyst showed a notable carbon yield to gases at 21 % in batch reactor, while the CuAl catalyst produced a minimal carbon yield to gases, below 1 %. In the fixed-bed reactor, the NiAlFe catalyst reached a carbon yield to liquids of 57.3 % and gases of about 13 %, whereas the NiAl catalyst achieved a lower carbon yield to liquids of 31.7 % and a yield to gases at around 10 %. Conversely, the CuAl catalyst had a carbon yield to liquids of around 8 % and gases of less than 1 %.

Analysis of the respective hydrogen yields revealed that the batch reactor delivered the highest hydrogen yield being higher for the NiAl catalyst than the NiAlFe catalyst, followed closely by the NiAlFe catalyst in the fixed-bed reactor. The CuAl catalyst gave the lowest H_2 yield among the three catalysts. Regarding liquid products, the NiAlFe catalyst primarily produced 1,2-PDO, achieving a selectivity of up to 65 % in both reactors. The NiAl catalyst exhibited a higher selectivity for 1,2-PDO and acetol in the fixed-bed reactor compared to the batch reactor. The CuAl catalyst's primary product was acetol, with higher selectivity in the batch reactor. These findings underscore the superior performance of the NiAlFe catalyst in glycerol APR, making it a promising candidate for hydrogen generation and co-production of valuable compounds. The inclusion of Fe in the NiAlFe catalyst appeared to have enhanced its catalytic activity, resulting in improved glycerol conversion and 1,2-PDO yield. Further optimisation of the reaction conditions for the NiAl and NiAlFe catalysts could help to tune the selectivity of the catalytic APR process toward producing more hydrogen and/or valuable chemicals.

CRediT authorship contribution statement

Carine T. Alves: Writing – original draft, Visualization, Validation, Methodology, Investigation, Funding acquisition, Data curation. **Francisco Maldonado-Martín:** Writing – original draft, Visualization, Validation, Methodology, Investigation, Data curation. **Alejandro Lete:** Writing – review & editing, Methodology, Investigation, Visualization. **Seyed Emad Hashemnezhad:** Writing – review & editing, Visualization, Validation, Methodology, Investigation, Data curation. **Lucía García:** Writing – review & editing, Writing – original draft, Visualization, Supervision, Project administration, Methodology, Funding acquisition, Conceptualization. **Jude A. Onwudili:** Writing – review & editing, Writing – original draft, Visualization, Supervision, Resources, Project administration, Methodology, Funding acquisition, Conceptualization.

Declaration of competing interest

The authors declare that they have no known competing financial interests or personal relationships that could have appeared to influence the work reported in this paper.

Acknowledgments

This work was supported by the EU Horizon Marie Curie Fellowship, Grant Number 892998 for C.T.A. and J.A.O. The authors (F.M-M., A.L. and L.G.) gratefully acknowledge financial support from Grants PID2020-114985RBI00 (funded by MICIU/AEI/10.13039/501100011033) and PID2024-160640OB-I00 (funded by MICIU/AEI/10.13039/501100011033 and ERDF/EU). Grant PRE2021-100578 funded by MICIU/AEI/10.13039/501100011033 and ESF+ awarded to F.M-M. Additional funding from the Government of Aragón through Research Group T22_23 R is also duly recognized.

Data availability

Data will be made available on request.

References

[1] B. Ayodele, T. Abdullah, M. Alsaffar, S. Mustapa, S. Salleh, Recent advances in renewable hydrogen production by thermo-catalytic conversion of biomass-derived glycerol: overview of prospects and challenges, Int. J. Hydrogen Energy 45 (36) (2020) 18160–18185, https://doi.org/10.1016/j.ijhydene.2019.08.002.

[2] D.L. King, L.A. Zhang, G. Xia, A.M. Karim, D.J. Heldebrant, X.Q. Wang, T. Peterson, Y. Wang, Aqueous phase reforming of glycerol for hydrogen production over Pt-Re supported on carbon, Appl. Catal. B Environ. 99 (1–2) (2010) 206–213, https://doi.org/10.1016/j.apcatb.2010.06.021.

[3] N. Roslan, S. Abidin, A. Ideris, D. Vo, A review on glycerol reforming processes over Ni-based catalyst for hydrogen and syngas productions, Int. J. Hydrogen Energy 45 (36) (2020) 18466–18489, https://doi.org/10.1016/j.ijhydene.2019.08.211.

[4] J.M. Silva, M.A. Soria, L.M. Madeira, Challenges and strategies for optimization of glycerol steam reforming process, Renew. Sustain. Energy Rev. 42 (2015) 1187–1213, https://doi.org/10.1016/j.rser.2014.10.084.

[5] I. Coronado, A. Arandia, M. Reinikainen, R. Karinen, R. Puurunen, J. Lehtonen, Kinetic modelling of the aqueous-phase reforming of fischer-tropsch water over Ceria-Zirconia supported nickel-copper catalyst, Catalysts 9 (11) (2019), https://doi.org/10.3390/catal9110936.

[6] Y. Wei, H. Lei, Y. Liu, L. Wang, L. Zhu, X. Zhang, G. Yadavalli, B. Ahring, S. Chen, Renewable hydrogen produced from different renewable feedstock by aqueous-phase reforming process, J. Sustain. Bioenergy Syst. 4 (2014) 113–127, https://doi.org/10.4236/jsbs.2014.42011.

[7] A. Minh, S. Samudrala, S. Bhattacharya, Valorisation of glycerol through catalytic hydrogenolysis routes for sustainable production of value-added C_3 chemicals: current and future trends, Sustain. Energy Fuels 6 (3) (2022) 596–639, https://doi.org/10.1039/d1se01333e.

[8] R. Davda, J. Shabaker, G. Huber, R. Cortright, J. Dumesic, Aqueous-phase reforming of ethylene glycol on silica-supported metal catalysts, Appl. Catal. B Environ. 43 (1) (2003) 13–26, https://doi.org/10.1016/S0926-3373(02)00277-1.

[9] I. Razaq, K. Simons, J. Onwudili, Parametric Study of Pt/C-Catalysed hydrothermal decarboxylation of butyric acid as a potential route for biopropane production, Energies 14 (11) (2021), https://doi.org/10.3390/en14113316.

[10] K. Tomishige, D. Li, M. Tamura, Y. Nakagawa, Nickel-iron alloy catalysts for reforming of hydrocarbons: preparation, structure, and catalytic properties, Catal. Sci. Technol. 7 (18) (2017) 3952–3979, https://doi.org/10.1039/c7cy01300k.

[11] R. Raso, A. Lete, L. Garcia, J. Ruiz, M. Oliva, J. Arauzo, Aqueous phase hydrogenolysis of glycerol with in situ generated hydrogen over Ni/Al_3Fe_1 catalyst: effect of the calcination temperature, RSC Adv. 13 (8) (2023) 5483–5495, https://doi.org/10.1039/d2ra07929a.

[12] R. Raso, E. Abad, L. García, J. Ruiz, M. Oliva, J. Arauzo, Renewable hydrogen production by aqueous phase reforming of Pure/Refined crude glycerol over Ni/Al-Ca catalysts, Molecules 28 (18) (2023), https://doi.org/10.3390/molecules28186695.

[13] C. Alves, J. Onwudili, Screening of nickel and platinum catalysts for glycerol conversion to gas products in hydrothermal media, Energies 15 (20) (2022), https://doi.org/10.3390/en15207571.

[14] R. Raso, L. Garcia, J. Ruiz, M. Oliva, J. Arauzo, Aqueous phase hydrogenolysis of glycerol over Ni/Al-Fe catalysts without external hydrogen addition, Appl. Catal. B Environ. 283 (2021), https://doi.org/10.1016/j.apcatb.2020.119598.

[15] A. Lete, R. Raso, L. García, J. Ruiz, J. Arauzo, Synthesis of ketones from glycerol and 1,2-propanediol using copper and nickel catalysts: unraveling the impact of reaction phase and active metal, Fuel 371 (2024), https://doi.org/10.1016/j.fuel.2024.132001.

[16] A. Lete, F. Lacleta, L. García, J. Ruiz, J. Arauzo, Effect of calcination temperature and atmosphere on the properties and performance of CuAl catalysts for glycerol dehydration to acetol, Biomass Bioenergy 195 (2025), https://doi.org/10.1016/j.biombioe.2025.107725.

[17] S.E. Hashemnezhad, J.A. Onwudili, K.E. Simons, P.E. Thornley, Kinetic and mechanistic studies of Pt/C-catalysed hydrothermal conversion of butyric acid for on-purpose production of renewable propane, Chem. Eng. J. 519 (2025) 165021, https://doi.org/10.1016/j.cej.2025.165021.

[18] S.E. Hashemnezhad, J.A. Onwudili, P. Thornley, K.E. Simons, Kinetics of hydrothermal reactions of n-butanol over Pt/Al_2O_3 catalyst for biopropane fuel gas production, Chem. Eng. J. 501 (2024) 157325, https://doi.org/10.1016/j.cej.2024.157325.

[19] J. Onwudili, I. Razaq, K. Simons, Optimisation of propane production from hydrothermal decarboxylation of butyric acid using Pt/C catalyst: influence of gaseous reaction atmospheres, Energies 15 (1) (2022), https://doi.org/10.3390/en15010268.

[20] F. Maldonado-Martín, L. García, J. Ruiz, M. Oliva, J. Arauzo, Selective conversion of glycerol to acetol: effect of the preparation method of CuAl catalysts and reaction phase, Catalysts 15 (4) (2025), https://doi.org/10.3390/catal15040348.

[21] R. Davda, J. Shabaker, G. Huber, R. Cortright, J. Dumesic, A review of catalytic issues and process conditions for renewable hydrogen and alkanes by aqueous-phase reforming of oxygenated hydrocarbons over supported metal catalysts, Appl. Catal. B Environ. 56 (1–2) (2005) 171–186, https://doi.org/10.1016/j.apcatb.2004.04.027.

[22] L. Garcia, A. Valiente, M. Oliva, J. Ruiz, J. Arauzo, Influence of operating variables on the aqueous-phase reforming of glycerol over a Ni/Al coprecipitated catalyst, Int. J. Hydrogen Energy 43 (45) (2018) 20392–20407, https://doi.org/10.1016/j.ijhydene.2018.09.119.

[23] P. Lozano, A. Simón, L. García, J. Ruiz, M. Oliva, J. Arauzo, Influence of the Ni-Co/Al-Mg catalyst loading in the continuous aqueous phase reforming of the bio-oil aqueous fraction, Processes 9 (1) (2021), https://doi.org/10.3390/pr9010081.

[24] J. Remon, J.R. Gimenez, A. Valiente, L. Garcia, J. Arauzo, Production of gaseous and liquid chemicals by aqueous phase reforming of crude glycerol: influence of operating conditions on the process, Energy Convers. Manag. 110 (2016) 90–112, https://doi.org/10.1016/j.enconman.2015.11.070.

[25] Z. Xiao, X. Wang, J. Xiu, Y. Wang, C. Williams, C. Liang, Synergetic effect between Cu^0 and Cu^+ in the Cu-Cr catalysts for hydrogenolysis of glycerol, Catal. Today 234 (2014) 200–207, https://doi.org/10.1016/j.cattod.2014.02.025.

[26] O. Diejomaoh, J. Onwudili, K. Simons, P. Maziero, On-purpose production of propane fuel gas from the hydrothermal reactions of n-butanol over Pt/Al_2O_3 catalyst: a parametric and mechanistic study, Fuel 365 (2024), https://doi.org/10.1016/j.fuel.2024.131140.

[27] E. Shkolnikov, N. Shaitura, M. Vlaskin, Structural properties of boehmite produced by hydrothermal oxidation of aluminum, J. Supercrit. Fluids 73 (2013) 10–17, https://doi.org/10.1016/j.supflu.2012.10.011.

[28] A. Adrianto, D. Denala, S. Jitkarnka, Partial substitution of promoters in Cu1.7[M]0.3Al-LDO (M=Ni, Mn, and Fe) catalysts for glycerol transformation to 1,2-propanediol, Catal. Today 461 (2026), https://doi.org/10.1016/j.cattod.2025.115536.

[29] R. Raso, L. Garcia, J. Ruiz, M. Oliva, J. Arauzo, Study of Ni/Al-Fe catalyst stability in the aqueous phase hydrogenolysis of glycerol, Catalysts 10 (12) (2020), https://doi.org/10.3390/catal10121482.

[30] M. D'Angelo, V. Ordomsky, J. van der Schaaf, J. Schouten, T. Nijhuis, Continuous hydrogen stripping during aqueous phase reforming of sorbitol in a washcoated microchannel reactor with a Pt-Ru bimetallic catalyst, Int. J. Hydrogen Energy 39 (31) (2014) 18069–18076, https://doi.org/10.1016/j.ijhydene.2014.02.167.